Transient X-ray Diffraction Reveals Global and Major Reaction Pathways for the Photolysis of Iodoform in Solution**

Jae Hyuk Lee, Joonghan Kim, Marco Cammarata, Qingyu Kong, Kyung Hwan Kim, Jungkweon Choi, Tae Kyu Kim, Michael Wulff, and Hyotcherl Ihee

The understanding of reaction mechanisms requires detailed information about the processes that take place during the reactions. Various time-resolved optical spectroscopic tools have been developed to track such processes, and reaction dynamics can now be routinely investigated, with a time resolution of tens of femtoseconds, by using these optical techniques.[1–12] Typical information provided by time-resolved spectroscopy includes the time constants of reaction intermediates and limited structural information. In most cases, however, detailed structural information, such as the bond lengths and angles in reaction intermediates, are extremely difficult to obtain from time-resolved optical spectroscopy (except for a few favorable cases in which they can be deduced from time-resolved vibrational spectroscopy[4–9] and multi-dimensional spectroscopy[10,11] measurements).

Replacing the optical probe pulses in time-resolved spectroscopy measurements with either electron[13–16] or X-ray pulses[17–22] converts the optical resonances in energy space into atomic interferences in real space, which offers a complementary—and more direct—way to investigate the structural dynamics of molecular reactions.[13–21] Because of the relatively low penetration depth of electrons, X-rays are more suitable for probing crystalline[23–25] and liquid samples;[17–20,22] for example, all the atoms in a protein can be tracked during its biological function by means of time-resolved X-ray crystallography,[23–25] but to do so it is necessary to produce single protein crystals. This limitation has been recently overcome by introducing transient X-ray liquidography (TXL), a method through which the transient molecular structures present in a liquid sample can be captured in one dimension by performing time-resolved X-ray diffraction measurements in the liquid phase.[17–22] TXL is a new technique that can be used to investigate reactions in solution, where most of the chemically and biologically relevant processes take place. Since the diffraction patterns generated by the short X-ray pulses arriving at the sample after laser excitation include all the molecular structures present in the irradiated volume, the analysis of TXL data can reveal the structural evolution of all the reaction pathways in the sample (limited only by the signal-to-noise ratio of the diffracted difference signal). We recently succeeded in studying the structural reaction dynamics of several molecules in solution by using this method.[17–22]

The photochemistry of iodoform (CHI_3) has received considerable attention because of the suggested formation of a unique intermediate, called isoiodoform (CHI_2-I), which has been studied by using several time-resolved spectroscopic methods, such as transient absorption and transient resonance Raman spectroscopies.[2,4] According to these studies, a parent iodoform molecule loses an iodine atom upon photo-excitation at 267 nm. The CHI_2 radical and the I atom then recombine geminately to form isoiodoform within the solvent cage; this is a common reaction in di- and trihaloalkanes.[2–4] Previous studies suggest that isoiodoform is the major intermediate, with a lifetime of several microseconds. We note that optical spectroscopy can be highly sensitive to a particular species, but sometimes this advantage translates into biased or nonglobal sampling, that is, certain intermediates might be optically "silent" and escape detection.[26] In contrast, the diffraction signal contains scattering information from all the atoms in the sample, thus providing a global picture of the reactions—although at the expense of sensitivity.[26] Herein we report the global dynamics of the photo-dissociation of iodoform in methanol and show that the formation of the isomer is not a major reaction channel in the investigated time range, that is, from 100 ps to 3 μs.

Time-resolved diffraction data were collected on the pump–probe beamline ID09B at the European Synchrotron Radiation Facility (ESRF) at time delays of −3 ns; −100, 100, and 300 ps; 1, 3, 6, 10, 30, 45, 60, 300, and 600 ns; and 1 and 3 μs. The diffraction signal corresponding the structural change is quite weak (about 0.1%) relative to the total diffraction signal. To extract the structural changes only, a non-excited reference data (at −3 ns) is subtracted from the diffraction data obtained at positive time delays. To magnify the scattered intensities at high angles (at which the signal becomes weak as a result of the decay in the atomic form factors), the change in the diffracted intensity, $\Delta S(q)$, is multiplied by $q = (4\pi/\lambda)\sin(\theta/2)$, where λ is the X-ray wave-

[*] J. H. Lee, J. Kim, K. H. Kim, Dr. J. Choi, Prof. H. Ihee
Center for Time-Resolved Diffraction
Department of Chemistry (BK21)
Korea Advanced Institute of Science and Technology (KAIST)
335 Gwahangno, Yuseong-gu, Daejeon 305–701 (Republic of Korea)
Fax: (+82) 42-869-2810
E-mail: hyotcherl.ihee@kaist.ac.kr
Homepage: http://time.kaist.ac.kr

Dr. M. Cammarata, Dr. Q. Kong, Prof. M. Wulff
European Synchrotron Radiation Facility
BP 220, Grenoble Cedex 38043 (France)

Prof. T. K. Kim
Department of Chemistry, Pusan National University
Geum Jeong Gu, Busan (Republic of Korea)

length and θ is the scattering angle. Figure 1 shows the difference intensities, $q\Delta S(q)$, and difference radial intensities, $r\Delta S(r)$, which represent the sine Fourier transform of the difference diffraction signals at each time delay. The latter
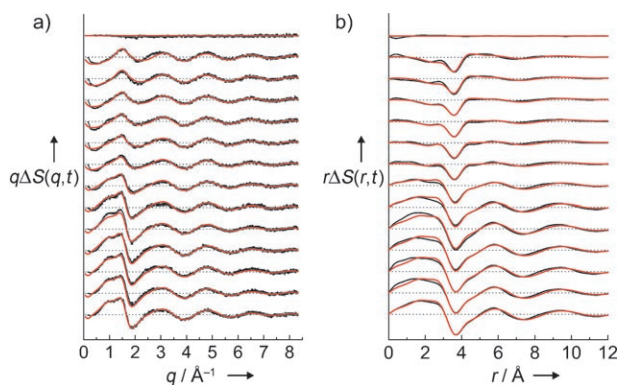

Figure 1. Time-resolved diffraction signal as a function of the time delay during the photolysis of iodoform in methanol. a) Difference diffraction intensities, $q\Delta S(q,t)$, excited minus nonexcited, at each time delay (black). The theoretical fits obtained from the global fitting analysis are shown in red. b) Corresponding difference radial intensities, $r\Delta S(r,t)$ (which represent the sine Fourier transformation of the difference diffraction intensities at each time delay).

pattern provides a more intuitive picture of the dynamics, whereby a positive peak means bond formation while a negative one means bond cleavage; for example, the prominent negative peak that appears at about 3.6 Å can be attributed to the decrease of the I−I distance in CHI$_3$ (mainly at short time delays and partly at longer time delays). The shoulder observed at 2.7 Å at late time delays can be partially attributed to the formation of a new I−I bond in I$_2$. Most positive and negative peaks located at distances larger than the size of the solute molecule are related to the solvent rearrangement, which results from temperature and density changes.[17–22] More detailed assignments are given in the Supporting Information.

We fitted the experimental difference intensities to theoretical values, thereby including changes from three components: 1) the solute-only term, 2) the solvent-only term (hydrodynamics), and 3) the solute–solvent cross term (cage). More details about the global fitting can be found in our previous publications.[17,18] The first term is simply the Debye scattering of isolated solute molecules (gas-phase diffraction contains only this term). Although molecular dynamics (MD) simulations can give us the second term, the sum of the temperature and density derivatives of the diffraction from the thermally excited solvent, the finite box size, and the approximate potentials involved in such simulations may lead to errors in the low-*q* region. A more accurate second term can be obtained experimentally by vibrationally exciting the pure solvent with near-infrared light.[22] MD simulations provide the third term. The time-independent structures of the solutes are obtained by means of density functional theory (DFT) calculations (Gaussian 03[27] with B3LYP/6-311++G-(d,p) for the C, H, and I atoms[28,29]). To account for the effect of the solvent on the structure of the solute molecule, the

integral equation formalism polarizable continuum model (IEFPCM)[30] was incorporated into the DFT calculation. The distances between two iodine atoms for the DFT-optimized structures of CHI$_3$ and the CHI$_2$ radical are 3.617 and 3.657 Å, respectively. The optimized isomer structure has three different distances between iodine atoms, namely, 3.616, 3.304, and 6.181 Å, and its C-I-I angle is 134°.

According to previous time-resolved spectroscopic studies,[2,3] the isomer CHI$_2$−I should be the main species (exhibiting a quantum yield of at least 0.5), with a rise time of 7 ps after the photodissociation of iodoform and a lifetime of hundreds of nanoseconds in nonpolar solvents (such as cyclohexane) and of microseconds in polar solvents (such as acetonitrile). To investigate the formation of this isomer, we performed global fitting analysis considering two possible reaction pathways, that is, the simple dissociation channel (CHI$_3$→CHI$_2$ + I) and the isomer formation channel (CHI$_3$→CHI$_2$−I). The χ^2 value of the isomer channel was nine times greater (at 10 ns) than that of the dissociation channel (Figure 2). Furthermore, when both reaction models were
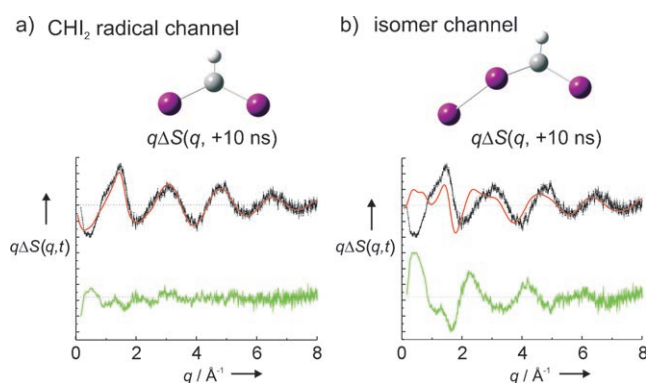

Figure 2. Time-resolved X-ray diffraction during the photolysis of iodoform in methanol. Top: The structures of two possible reaction pathways are shown purple I, gray C, white H: a) the simple dissociation channel (CHI$_3$→CHI$_2$ + I) and b) the isomer formation channel (CHI$_3$→CHI$_2$−I). The structures of the radical and the isomer were obtained from DFT calculations. Bottom: Comparison of the experimental difference diffraction curves [$q\Delta S(q,+10\ ns)$] at 10 ns (black) with the corresponding theoretical curves (red) obtained from global fitting studies performed considering two possible reaction pathways: a) radical formation and b) isomer formation. The results confirm that simple dissociation is the major reaction pathway.

included in the fit, the fraction of the isomer-formation process converged to zero. In addition to the optimized isomer structure, which has a C-I-I angle of 134°, other isomer structures with C-I-I angles ranging from 134 to 90° were also tested. However, none of them fitted our experimental data (see the Supporting Information). These results indicate that the isomer formation is not a major channel (between 100 ps and 3 µs) in our experiments. Although the solvent (methanol) used in this work is slightly different from those employed in previous studies, we note that the isomer was reported for both polar and nonpolar solvents. Methanol, whose dielectric constant is about 33, should correlate well with acetonitrile (which has a dielectric constant of 37). In

terms of viscosity, methanol (whose viscosity is 0.59 cP) lies between acetronitrile (0.38 cP) and cyclohexane (1.0 cP). In previous time-resolved optical spectroscopic studies, in which the *iso*-CHI$_3$ species was observed, the excitation wavelengths were 310, 350, and 370 nm, whereas we used 266 nm in this work. The low-lying absorption bands (including that at 266 nm, which was used in our work) arise from the n(I)→σ*(C−I) transition. In the case of CH$_2$I$_2$, the intermediate *iso*-CH$_2$I$_2$ was suggested to be formed, regardless of the excitation wavelength (266, 310, and 350 nm). Therefore, it is likely that the same species would form, regardless of the excitation wavelength, as far as the n(I)→σ*(C−I) transition is concerned.

Figure 3 shows a schematic of the reaction mechanism determined in this study. Upon excitation with a 266-nm laser pulse, iodoform promptly dissociates into a CHI$_2$ radial and a neutral I atom. Molecular iodine (I$_2$) is then formed by means
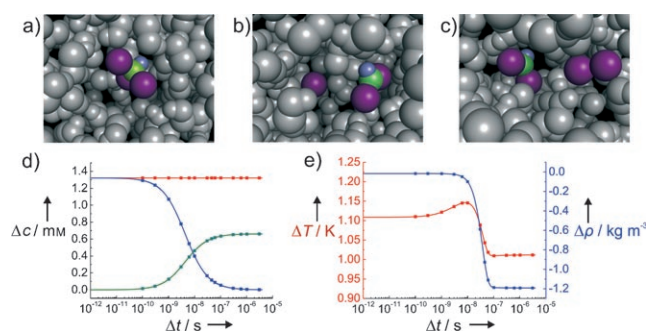

Figure 3. Reaction mechanism and reaction kinetics of the photolysis of iodoform in methanol (determined by TXL). a) Iodoform in methanol before laser initiation. b) Upon irradiation, the CHI$_2$ radical and an I atom are produced. c) After 100 ns, molecular iodine (I$_2$) is formed by nongeminate recombination. Purple I, green C, blue H. d) Concentration profiles of the relevant chemical species as a function of the time delay (the measured time delays are indicated with symbols); red CHI$_2$, blue I, green I$_2$. e) Changes in the temperature (red) and the density (blue) of the bulk solvent. The initial temperature rise is a result of ultrafast geminate (in-cage) recombination. All results were obtained by global fitting of the diffraction patterns.

of a nongeminate recombination of two iodine atoms, which takes about 100 ns, as shown in Figure 3c. However, the formation of the isomer (CHI$_2$−I) was not detected at times shorter than a few microseconds. From the global fitting of the time-resolved diffraction signal, we can determine the spatiotemporal photoreaction kinetics for iodoform (Figure 3d). The rate constant for the nongeminated recombination of I$_2$ molecules is $(3.1 \pm 0.5) \times 10^{10} \, \text{M}^{-1} \text{s}^{-1}$. This value is close to that found in CCl$_4$ solutions by optical spectroscopy.[31] Neither the formation of CHI$_3$ through the nongeminate recombination of CHI$_2$ and I nor the production of CHI$_2$−CHI$_2$ from two CHI$_2$ radicals were observed. The predominance of I$_2$ formation over other possibilities can be partly understood by considering that CHI$_2$ diffuses slower than I and that the nongeminate recombination of I$_2$ can occur regardless of the approaching direction of two partners.

The time-dependent changes in solvent density and temperature provide information about the hydrodynamics

of the solvent, which is mathematically linked to the solute kinetics through the conservation of the heat released from the solute to the surrounding solvent. Initially, the temperature and the pressure of the solvent increase—at constant volume—as a result of an energy transfer from the solute to the solvent. Then, thermal expansion occurs (with a time constant of about 50 ns), which returns the sample to ambient pressure. As a result of the thermal expansion, the density of the solvent decreases by 1.2 kg m^{-3} (0.15%) at 1 μs, which corresponds to a temperature increase of 1.02 K.

In conclusion, we investigated the structural dynamics of the photodissociation of iodoform in methanol by means of TXL. Upon photoexcitation of iodoform with 2-ps laser pulses (at 266 nm), the iodoform molecule quickly dissociates into a CHI$_2$ radical and an I atom, followed by the nongeminate formation of I$_2$ from two iodine atoms. No CHI$_3$ or CHI$_2$−CHI$_2$ species were detected. The solvent's response to the reaction was revealed by density and temperature changes observed as a function of time. While spectroscopic studies reported the existence of isoiodoform (which forms within 7 ps and has a lifetime of several microseconds), our time-resolved diffraction data did not show any signals for this species within the studied time-delay range (that is, between 100 ps and 3 μs). Since the X-ray pulse width used in this study was approximately 100 ps (full width at half maximum, fwhm), the formation of isoiodoform as a major species on timescales shorter than our experimental time resolution cannot be ruled out.

Experimental Section

Time-resolved X-ray diffraction was performed on the beamline ID09B at the ESRF. A solution of iodoform in methanol (20 mM) was used to collect the data. This solution was circulated through the sapphire nozzle to form a stable 300-μm-thick liquid layer, which was directly exposed to the laser/X-ray beams. A 150-fs laser pulse (at 800 nm) was converted to the third harmonic (266 nm) and then stretched to 2 ps in a prism to avoid multiphoton effects. The laser pulses were synchronized with the X-ray pulses at a repetition rate of 986.3 Hz. After excitation of the iodoform sample with the laser pulse, delayed 100-ps-long X-ray pulses (generated by a low-K monoharmonic undulator, the U17) delivered 5×10^8 photons per pulse on the sample (in a 3% relative bandwidth around the wavelength 0.68 Å). The diffraction patterns were collected using a MarCCD X-ray detector system (with a 133 mm diameter). More details are provided in our previous publications.[17, 18, 22]

[1] A. H. Zewail, *Angew. Chem.* **2001**, *113*, 4501; *Angew. Chem. Int. Ed.* **2001**, *40*, 4371.

[2] X. M. Zheng, D. L. Phillips, *Chem. Phys. Lett.* **2000**, *324*, 175.

[3] M. Wall, A. N. Tarnovsky, T. Pascher, V. Sundstrom, E. Akesson, *J. Phys. Chem. A* **2003**, *107*, 211.

[4] Y. L. Li, D. M. Chen, D. Q. Wang, D. L. Phillips, *J. Org. Chem.* **2002**, *67*, 4228.

[5] N. Biswas, S. Umapathy, *J. Chem. Phys.* **1997**, *107*, 7849.

[6] P. Kukura, D. W. McCamant, S. Yoon, D. B. Wandschneider, R. A. Mathies, *Science* **2005**, *310*, 1006.

[7] Y. Mizutani, T. Kitagawa, *Science* **1997**, *278*, 443.

[8] W. J. Schreier, T. E. Schrader, F. O. Koller, P. Gilch, C. E. Crespo-Hernandez, V. N. Swaminathan, T. Carell, W. Zinth, B. Kohler, *Science* **2007**, *315*, 625.

[9] S. O. Williams, D. G. Imre, *J. Phys. Chem.* **1988**, *92*, 3363.

[10] H. Lee, Y. C. Cheng, G. R. Fleming, *Science* **2007**, *316*, 1462.

[11] J. R. Zheng, K. W. Kwak, J. Xie, M. D. Fayer, *Science* **2006**, *313*, 1951.

[12] D. H. Paik, I. R. Lee, D. S. Yang, J. S. Baskin, A. H. Zewail, *Science* **2004**, *306*, 672.

[13] H. Ihee, V. A. Lobastov, U. M. Gomez, B. M. Goodson, R. Srinivasan, C. Y. Ruan, A. H. Zewail, *Science* **2001**, *291*, 458.

[14] R. C. Dudek, P. M. Weber, *J. Phys. Chem. A* **2001**, *105*, 4167.

[15] S. T. Park, J. S. Feenstra, A. H. Zewail, *J. Chem. Phys.* **2006**, *124*.

[16] B. J. Siwick, J. R. Dwyer, R. E. Jordan, R. J. D. Miller, *Science* **2003**, *302*, 1382.

[17] H. Ihee, M. Lorenc, T. K. Kim, Q. Y. Kong, M. Cammarata, J. H. Lee, S. Bratos, M. Wulff, *Science* **2005**, *309*, 1223.

[18] T. K. Kim et al., *Proc. Natl. Acad. Sci. USA* **2006**, *103*, 9410. see the Supporting Information.

[19] M. Wulff, S. Bratos, A. Plech, R. Vuilleumier, F. Mirloup, M. Lorenc, Q. Kong, H. Ihee, *J. Chem. Phys.* **2006**, *124*, 034501.

[20] A. Plech, M. Wulff, S. Bratos, F. Mirloup, R. Vuilleumier, F. Schotte, P. A. Anfinrud, *Phys. Rev. Lett.* **2004**, *92*, 125505.

[21] a) J. Davidsson et al., *Phys. Rev. Lett.* **2005**, *94*, 245503. see the Supporting Information; b) J. H. Lee, K. H. Kim, T. K. Kim, Y. Lee, H. Ihee, *J. Chem. Phys.* **2006**, *125*, 174504.

[22] M. Cammarata, et al., *J. Chem. Phys.* **2006**, *124*, 124504. see the Supporting Information.

[23] H. Ihee, S. Rajagopal, V. Srajer, R. Pahl, S. Anderson, M. Schmidt, F. Schotte, P. A. Anfinrud, M. Wulff, K. Moffat, *Proc. Natl. Acad. Sci. USA* **2005**, *102*, 7145.

[24] V. Schmidt, R. Pahl, V. Srajer, S. Anderson, Z. Ren, H. Ihee, S. Rajagopal, K. Moffat, *Proc. Natl. Acad. Sci. USA* **2004**, *101*, 4799.

[25] F. Schotte, M. H. Lim, T. A. Jackson, A. V. Smirnov, J. Soman, J. S. Olson, G. N. Phillips, M. Wulff, P. A. Anfinrud, *Science* **2003**, *300*, 1944.

[26] R. Srinivasan, J. S. Feenstra, S. T. Park, S. J. Xu, A. H. Zewail, *Science* **2005**, *307*, 558.

[27] Gaussian 03 (Revision A.1), M. J. Frisch et al., see the Supporting Information.

[28] M. N. Glukhovtsev, A. Pross, M. P. Mcgrath, L. Radom, *J. Chem. Phys.* **1995**, *103*, 1878.

[29] A. Strömberg, O. Gropen, U. Wahlgren, *J. Comput. Chem.* **1983**, *4*, 181.

[30] E. Cances, B. Mennucci, J. Tomasi, *J. Chem. Phys.* **1997**, *107*, 3032.

[31] S. Aditya, J. E. Willard, *J. Am. Chem. Soc.* **1957**, *79*, 2680.